RSC Advances

This is an *Accepted Manuscript*, which has been through the Royal Society of Chemistry peer review process and has been accepted for publication.

Accepted Manuscripts are published online shortly after acceptance, before technical editing, formatting and proof reading. Using this free service, authors can make their results available to the community, in citable form, before we publish the edited article. This *Accepted Manuscript* will be replaced by the edited, formatted and paginated article as soon as this is available.

You can find more information about *Accepted Manuscripts* in the Information for Authors.

Please note that technical editing may introduce minor changes to the text and/or graphics, which may alter content. The journal's standard Terms & Conditions and the Ethical guidelines still apply. In no event shall the Royal Society of Chemistry be held responsible for any errors or omissions in this *Accepted Manuscript* or any consequences arising from the use of any information it contains.

ROYAL SOCIETY OF CHEMISTRY

www.rsc.org/advances

A novel CdS photocatalyst based on magnetic fly ash cenospheres as the carrier: Performance and mechanism

Ming He,[a] Ziyang Lu,[b] Weichao Zhou,[c] Tingting Chen,[b] Weidong Shi,[a] Guangbo Che,[a,d] Pengwei Huo,[a] Zhi Zhu,[a] Xiaoxu Zhao [a] and Yongsheng Yan *[a]

[a] School of Chemistry and Chemical Engineering, Jiangsu University, Zhenjiang 212013, PR China

[b] School of The Environment and Safety Engineering, Jiangsu University, Zhenjiang 212013, PR China

[c] School of Material Science and Engineering, Jiangsu University, Zhenjiang 212013, PR China

[d] College of Environmental Science and Engineering, Jilin Normal University, Siping 136000, PR China

Abstract

A novel magnetic photocatalyst CdS/MFACs were synthesized by chemical deposition with direct growth of CdS nanoparticles on the surface of MFACs. The photodegradation of danofloxacin mesylate (76.2%) demonstrated that CdS/MFACs exhibited higher photocatalytic activity than that of pure CdS (71.5%) under the irradiation of visible light. Moreover, this as-prepared photocatalyst was relatively stable and displayed a good reusability after 5 cycles. The reasonable photocatalytic mechanism over CdS/MFACs was verified by the reactive species trapping and further confirmed by ESR technique as well as employed a radicals scavenging species–DMPO. Furthermore, the hydroxyl radicals qualitative analysis of experiments showed that ·OH was existed in the photocatalytic degradation process and only generated from the photogenerated electrons on the conduction band of CdS/MFACs. And the experimental results showed that the photodegradation of danofloxacin mesylate is associated with $\cdot O_2^-$ and photogenerated holes. Finally, the photocatalysis degradation reaction kinetics and the mechanism of photodegradation of danofloxacin mesylate were also discussed.

Key words: CdS photocatalyst; Magnetic fly-ash; Spin trapping; Radical quenchers; Mechanism

1. Introduction

Antibiotics are increasingly found in the environment and have attracted much attention. Although the concentration of antibiotics residue in the aquatic environment is low, it is widely recognized that antibiotic pollution contributes to antibiotic resistance dissemination [1]. Moreover, because of its inhibitory for biomass growth, it is hard to be degraded via traditional biological process. Thus, specific treatments have been used to remove antibiotics from wastewater, such as adsorption [2], ultrasonic degradation [3], electrolysis [4]. However, these approaches are incomplete and energy-inefficient. Photocatalytic technology is considered as an advanced oxidation processes in environmental protection and energy, which is also extensively applied to remove of medical organic pollutants [5, 6]. P25 is one kind of the most extensively studied semiconductors. But the wide band gap of P25 limits the practical application in the case of solar light. Therefore, it is extremely necessary to develop the visible-light-driven photocatalysts for the use of solar energy. CdS is an important II−VI semiconductor with a direct band gap of 2.4 eV. Owing to its unique properties mentioned above, CdS is widely used in the field of solar cells [7], photoelectric conversion [8], photocatalytic application [9], photo-splitting water [10], etc. Hao et al. [11] reported the

RSC Advances Accepted Manuscript

preparation of CdS nanorings by chemical bath deposition, and this as-prepared CdS nanorings exhibited a high photocatalytic efficiency in the degradation of rhodamine. Singh et al. [12] synthesized CdS nanorods via solvothermal technique and investigated the photocatalytic degradation of salicylic acid. Nevertheless, all of these pure CdS are difficult to recycle and the utilization rates are low. It is reported that immobilizing the catalysts on a support can overcome these problems [13, 14], and improve utilization rate of photocatalyst is an efficient method. The primary reason is that the photocatalytic reaction often occurs on the surface of the catalyst, which is directly exposed to light and the reactants. Consequently, a number of research works has been done for loading CdS on other materials to increase the photocatalytic efficiency and immobility of the catalysts, the common materials including CNTs [15], SiO_2 [16], polymer [17] and halloysite nanotubes (HNTs) [18]. However, the aforementioned supports have high cost and are difficult to obtain, which restrict their widely applications.

Fly ash cenospheres (FACs) is a by-product generated in coal-fired power plants. This compose of microscopic flakes and cenospheres of mullite, which is considered to have great potential application for catalyst supported material with excellent corrosion resistance, high thermal stability [19]. For this particular reason, some composite photocatalysts prepared by coating photocatalysts onto the surface of FACs have also been reported [20, 21]. In order to recycling catalyst, magnetic composite prepared by coating a magnetic Fe_3O_4 layer onto the surface of FACs had been reported [22]. However, this method is complex and inefficient. As one kinds of FACs, Magnetic fly ash cenospheres (MFACs) can be easily recycled and reused for several times efficiently, because of its magnetic propertities owe to the presence of iron oxides.

For photocatalytic mechanism of CdS, a number of researchers have reported the detection and identification of various radicals formed on CdS during the photocatalytic process. Active oxygen species such as hydroxyl radicals (·OH) [23], superoxide radicals ($\cdot O_2^-$) [24] and photogenerated holes (h^+) [25] have been regarded as key species. However, the detailed process of the consumption of radicals is still a controversial issue. For instance, Gao et al. reported that the photogenerated holes of CdS participate in the redox reactions to form ·OH in the photocatalytic process. Nevertheless, the VB edge potential of CdS was more negative than the standard redox potentials of $\cdot OH/OH^-$ (+2.38 eV). It is theoretically speculated that the photogenerated holes cannot result in the formation of hydroxyl radicals. Currently, to our knowledge, there are few investigations have been reported on this subject by using electron spin resonance (ESR) spectroscopy [26].

In this study, the CdS/MFACs composites were synthesized by chemical bath deposition with direct loaded CdS on the surface of MFACs. The obtained composites were characterized by X-ray diffraction (XRD), scanning electron microscope (SEM) and UV−vis diffuse reflectance spectra (UV−vis DRS), the photocatalytic performance in degradation and mineralization of danofloxacin mesylate under the visible light irradiation was investigated. Moreover, we use radical inhibitors during photocatalytic process to research the effects of radical on photocatalytic activity. In particular, the hydroxyl radicals generated from photocatalytic process were studied using fluorescence and ESR spectrum. The photodegradation mechanism of danofloxacin mesylate was also discussed through the mass spectrum (MS), the results indicated that danofloxacin mesylate was degraded step by step and finally decomposed to CO_2, H_2O and other gaseous components.

2. Materials and method

2.1. Materials and reagents

RSC Advances Accepted Manuscript

Hydrogen chloride (HCl, 37%), ethanol (CH_3CH_2OH), methanol (CH_3OH), methylbenzene (C_7H_8), N,N-dimethylformamide (DMF), thiourea (NH_2CSNH_2), ammonia solution ($NH_3•H_2O$), tert-butyl alcohol (tBuOH), triethanolamine (TEOA) were purchased from Sinopharm Chemical Reagent Co., Ltd. (Shanghai, China). Succinic anhydride, coumarin, (3-aminopropyl) triethoxysilane (APTES)，cadmium sulfate, 8/3-hydrate ($CdSO_4•8/3H_2O$), dimethyl sulfoxide (DMSO), 5,5-dimethyl-1-pyrroline N-oxide (DMPO), were purchased from Aldrich. All the reagents were analytical grade and used as received, without further purification.

2.2. Synthesis of CdS/MFACs

Screening and modifying magnetic fly ash cenospheres: The fly ash used in this study was collected from the cyclone of a mass-burning incinerator located in the city of Pingdingshan (China). Due to the fact that the iron ore was existed in some raw materials, hence, some magnetic fly ash cenospheres possessed the magnetism, and the magnetism was conducive to the recycle of the photocatalyst. The details of the procedure for the preparation of CdS/MFACs were shown in Scheme 1. First of all, 30 μm - 50 μm magnetic fly ash cenospheres (MFACs) were selected using different mesh size of screen. After 5 g MFACs were mixed in 120 ml 1 mol L^{-1} HCl, this mixture was stirred for 3 h at a constant temperature of 80 ˚C. Afterwards, the product was washed with deionized water to neutral and dried under vacuum at room temperature, acid-activated MFACs were obtained. In the following step, 3 g acid-activated MFACs and 10ml APTES were added into 120 ml methylbenzene, this mixture was stirred for 12 h at 70 ˚C under a nitrogen atmosphere. After the product was washed with methylbenzene and methanol for three times, amino modified MFACs (NH_2-MFACs) were obtained. At last, in order to obtain carboxyl modified MFACs (COOH-MFACs), 2 g NH_2-MFACs and 3 g succinic anhydride were added into 50 ml DMF with mechanical agitation for 24 h at room temperature. Subsequently, the solid product was washed with DMF and ethanol for three times and dried under vacuum at room temperature for 12 h.

Synthesis of CdS/MFACs photocatalyst: In a typical synthetic process, 0.5 g COOH-MFACs were well-dispersed in deionized water (80 ml) within magnetic stirring, afterward $CdSO_4$ (2 mmol), thiourea (4 mmol) and ammonia (5 g) were added into above suspension. The mixture was kept at 60 ˚C with vigorously magnetic stirring for 3 h. After the reaction, the solid sample was washed with deionized water and ethanol for three times and under vacuum at 30 ˚C for 3 h. The reaction process can be described as follows:

$$Cd(NH_3)_n^{2+} + SC(NH_2)_2 + 2OH^- \rightarrow CdS + 2H_2O + CN_2H_2 + 2nNH_3$$

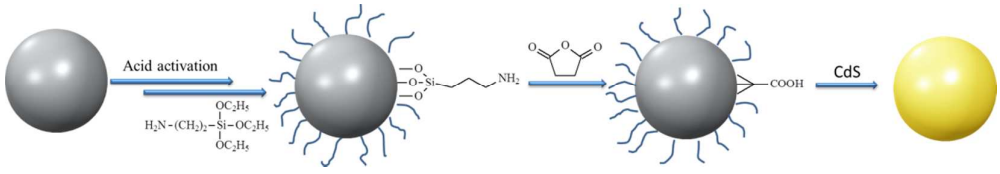

Scheme.1. Illustration of the preparation of CdS/MFACs

2.3. Adsorption experiment

The danofloxacin mesylate solution (20 mg L^{-1}) was used as a target pollutant. 20 mg photocatalyst was added into 100 mL danofloxacin mesylate solution. The samples were conducted at the thermostatic bath with magnetically stirring at 30 ˚C for 2h. The concentration of free danofloxacin mesylate in the solution was measured at 275 nm by a UV-vis spectrophotometer. The adsorption capacity (Q) was calculated as follows:

RSC Advances Accepted Manuscript

$$Q = \frac{(C_0 - C)V}{W}$$

where C_0 (mg L^{-1}) is the initial concentration of danofloxacin mesylate, C (mg L^{-1}) is the residual concentration of danofloxacin mesylate in solution, V (L)is the volume of danofloxacin mesylate solution, W (g) is the mass of photocatalysts, and Q (mg g^{-1}) is the absorbed amount

2.4. Evaluation method of photocatalytic activity

The activity of photocatalysts was evaluated by degrading danofloxacin mesylate under the visible light irradiation. In experiments, 0.02 g photocatalyst and 100 ml danofloxacin mesylate solution were added into photocatalytic reaction flask, the reaction was conducted at the thermostatic bath with magnetically stirring at 30 °C using a 250 W xenon lamp (Philips MSD 250) as the light source. The xenon lamp was placed at 10 cm distance parallel to the reaction flask, and the light below 420 nm was filtered by a glass optical filter. Before the photocatalytic degradation, the suspensions were magnetically stirred in dark reach the adsorption equilibrium. For monitoring the photocatalytic process, 7 ml of danofloxacin mesylate solution were taken out from the reaction flask interval of 10 min and analyzed by a UV-vis spectrophotometer at 275 nm.

In the recycle experiments, the catalysts were separated initial three times by deionized water and ethanol for several times to remove the residual danofloxacin mesylate and degradation by-products, afterwards, the catalysts was re-dispersed in the danofloxacin mesylate solution (100 mL, 20 mg L^{-1}) for another cycle.

2.5. Detection method of active oxygen species.

In order to detect the hydroxyl radicals (·OH), holes (h^+) and superoxide radicals ($\cdot O_2^-$) in the danofloxacin mesylate solution, these radicals probably worked as the active species during photocatalytic reactivity, 1.0 mM tBuOH (a quencher of ·OH), 1 mM TEOA (a quencher of h^+) and nitrogen (2 L min^{-1}) (to replace air) into danofloxacin mesylate solution, respectively, followed by the photocatalytic activity test. In addition, the formation of ·OH radicals was also evaluated by using coumarin as a fluorescence probe, coumarin reacts more easily with ·OH to form highly fluorescent 7-hydroxycoumarin. Instead of danofloxacin mesylate, coumarin (1.0 mmol L^{-1}) was added into the systems of CdS/MFACs. The fluorescent intensity of generated 7-hydroxycoumarin was monitored at 456 nm with the excitation wavelength of 346 nm on a VARIAN cary Eclipse spectrofluorometer.

2.6. Characterization

Phases and atomic concentrations of different elements were investigated using a Bruker D 8 advance powder XRD System with a Cu Kα (λ=1.5418 Å) radiation source. Diffraction patterns were collected from 20° to 70° at a speed of 5° min^{-1}. The surface morphology and the detailed crystal structure of the synthesized CdS/MFACs were analyzed by using a field emission scanning electron microscope (SEM) (JSM-7001F) equipped with energy-dispersive spectroscopy analysis (EDS). The UV−vis diffuse reflectance spectra (UV−vis DRS) of the samples were recorded by UV 2450 spectrophotometer in the range of 200 nm−800 nm. Nitrogen physisorption was detected by a Quantachrome micromeritics NOVA 2000e. The adsorption and desorption isotherms were analyzed using the Brunauer. Emmett. Teller (BET) and the specific surface area and pore size distribution were calculated by Barrett–Joyner–Halenda (BJH) methods, respectively. The Raman spectra were collected at room temperature using a Thermo Scientific DXR Raman spectrometer. Thermal gravimetric (TG) analysis were figured out in a thermo gravimetric analyzer (STA449C, NETZSCH). Photoluminescence (PL) spectra were performed at room temperature with a

RSC Advances Accepted Manuscript

VARIAN cary Eclipse spectrofluorimeter. Total organic carbon (TOC) analysis was performed on a TOC/TN analyzer multi N/C 2100/2100 S. The degradation course of danofloxacin mesylate solution was detected by the Thermo LXQ mass spectrometry (MS). Active free radicals were identified with electron spin resonance (ESR) on a JEOL FA-200. For the measurement, the samples (100 μl) were collected from the reaction solution after being reacted for 4 min, and immediately mixed with 20 μl DMPO (20 mmol L^{-1}) to form DMPO-radicals adduct. Because of the instability in water solutions, the ESR signal of $\cdot O_2^-$ was detected by dimethyl sulfoxide.

3. Results and discussion

3.1 Surface morphology

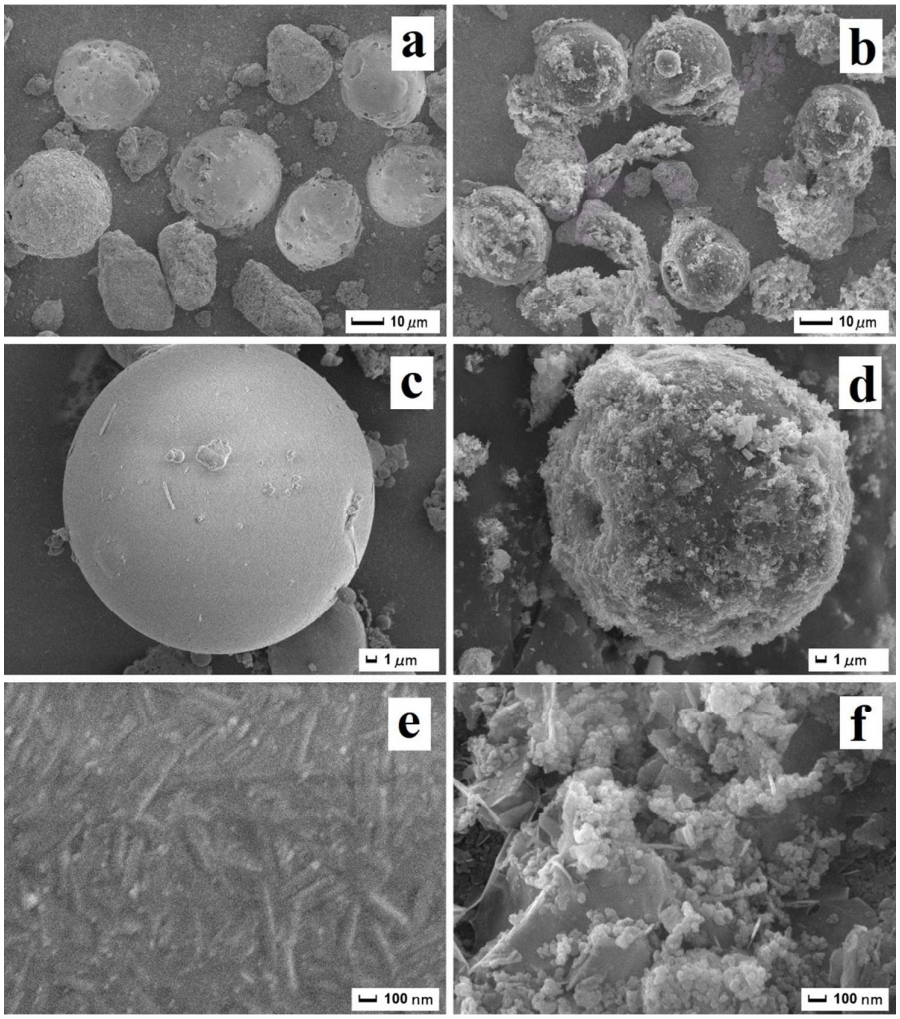

Fig. 1. SEM images of different photocatalysts: MFACs (a,c), amplify of MFACs (e), CdS/MFACs (b,d), amplify of CdS/MFACs (f)

The morphologies of the catalysts were observed via SEM. Fig. 1a–f shows typical SEM images of the MFACs and CdS/MFACs, respectively. Fig. 1a, c and e presents a typical SEM image of the MFACs which were regular sphere with diameter of approximately 30 μm. Moreover there were little impurity on the surface and a hollow spherical shape (Fig. S2). Compared with the smooth surface showed in the Fig. 1e, it could be clearly seen in the Fig. 2b, d and f that the surfaces of MFACs were become rough by covered with a great amount of particles and scales. These results indicated that CdS nanoparticles have been successfully deposited on the surfaces of

RSC Advances Accepted Manuscript

the MFACs. Fig. S1 shows the EDS patterns of CdS/MFACs which revealed the elements of main chemical composition of MFACs (SiO_2, Al_2O_3) and CdS loading on the surface of MFACs. Particularly, the Fe peak was mainly caused by the iron oxides in the MFACs.

3.2 Crystal structure

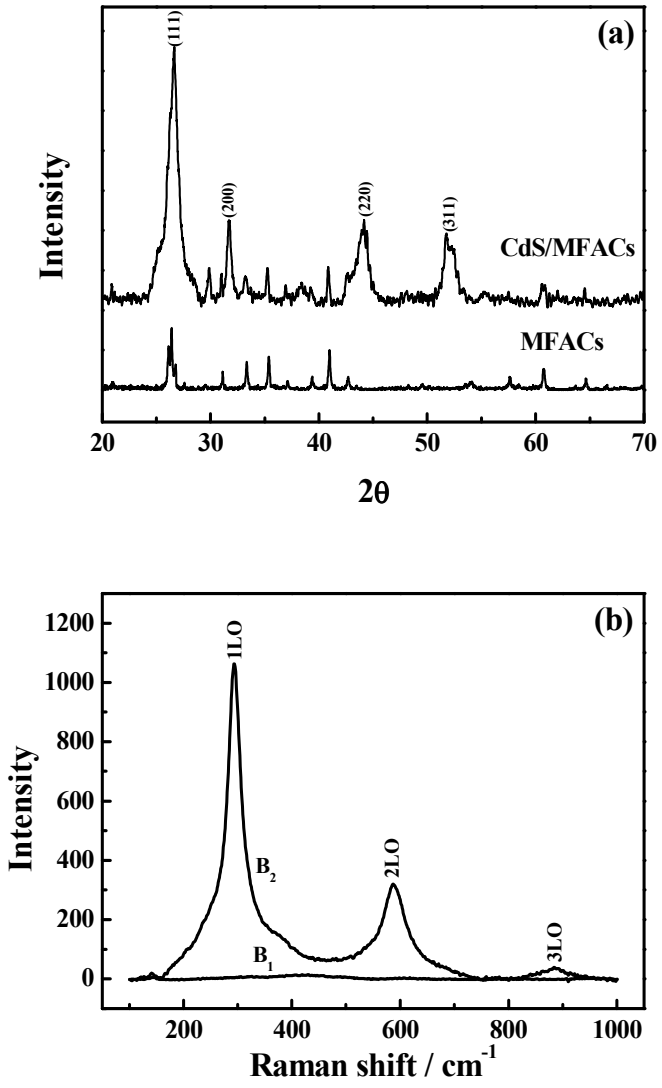

Fig. 2. XRD patterns of the CdS/MFACs photocatalysts (a) and micro Raman spectra of MFACs and CdS/MFACs (b)

Fig. 2a shows the XRD patterns of MFACs and CdS/MFACs photocatalysts characteristic diffraction peaks of MFACs can be obviously seen in the pattern of MFACs, which were well matched with the results reported [27], while a sharp and high peak of nanocrystallite CdS could be viewed in the XRD pattern of CdS/MFACs. The peaks around 2θ of 26.46°, 31.67°, 44.09°and 51.75° are corresponding to the characteristic peaks (111), (200), (220), and (311) of CdS (JCPDS 01-0647), which means that CdS has been successfully coated on the surface of MFACs, which was in a good agreement with the result of SEM.

It is well known that vibrational spectroscopy is a useful tool for examining the crystal phase.

RSC Advances Accepted Manuscript

Raman spectroscopy of semiconductors is a fast, nondestructive tool to evaluate crystalline material qualities including surface conditions and homogeneity. Fig. 2b shows the micro Raman spectra of MFACs and CdS/MFACs at room temperature. There are no obvious peaks in Raman spectra of MFACs (line B_1). While three peaks at 293.1 cm^{-1}, 587.2 cm^{-1} and 892.8 cm^{-1} in Raman spectra of CdS/MFACs(line B_2), which corresponding to the first-order, second-order and three-order longitudinal optical phonon (LO) modes of CdS, respectively, which was in good agreement with previous report on CdS nanostructures [28].

3.3 UV-vis spectra of photocatalysts

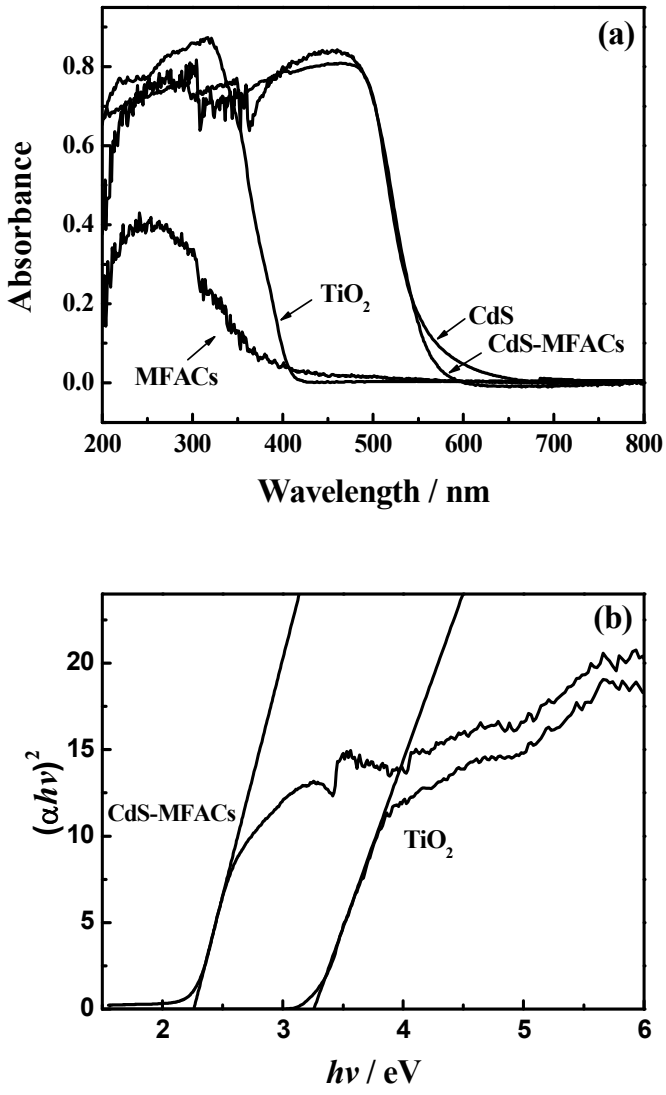

Fig. 3. UV–vis reflectance absorption spectra of photocatalysts (a) and band gap energies of photocatalysts (b).

Fig. 3a shows the diffuse reflectance absorption spectra of MFACs, P25, CdS and CdS/MFACs. According to this figure, MFACs had a weak absorption between 200 nm to 380 nm in the ultraviolet region. In contrast, CdS/MFACs showed a broad absorption throughout the ultraviolet light region. And the absorption edge shifted towards the longer wavelength side

RSC Advances Accepted Manuscript

compared with P25. Moreover, CdS/MFACs had intensive absorptions presented in visible range of about 400 nm – 550 nm. Promoted organic pollutions degradation under visible light. The absorption was almost disappeared when the wavelength over 600 nm. The sharp absorption started at the wavelength of 520 nm indicated no absorption of impurity energy levels and mainly resulted from the band-gap transition of electrons from the valance band to the conduction band of CdS. In addition, Tauc's relationship for optical band-gap calculations of the photocatalysts was described as:

$$(\alpha hv)^n = k(hv - E_g)$$

Where α is the absorption coefficient, k is the parameter that to the effective masses associated with the valence and conduction bands, n is 2 for a direct transition, hv is the absorption energy, E_g is the band gap energy [29]. Fig. 3b shows Tauc's plot for the CdS systems. It revealed that $(\alpha hv)^2$ was plotted against the photon energy (hv) and the band gaps were 2.26 eV for free CdS/MFACs, 3.26 eV for P25, which were estimated from the extrapolated Tauc's plot.

3.4 BET and VSM of composite photocatalysts

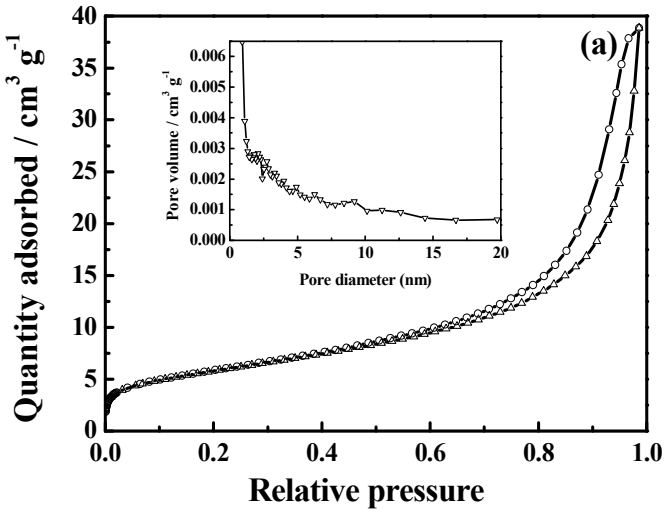

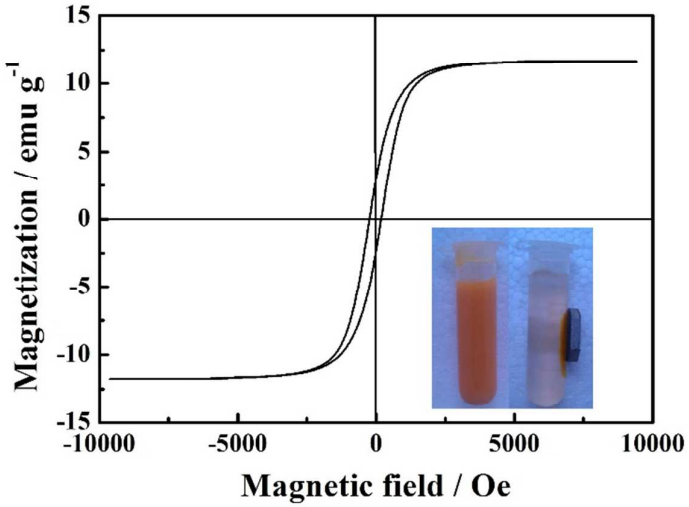

RSC Advances Accepted Manuscript

Fig. 4. Nitrogen adsorption/desorption isotherm and Barrett–Joyner–Halenda (BJH) pore size distribution plot (inset) of the CdS/MFACs (a) and magnetization curves of CdS/MFACs (b)

Brunauer–Emmett–Teller (BET) gas sorptometry measurements had been conducted to examine the adsorption–desorption isotherms and the pore-size distribution (inset) of the CdS/MFACs as shown in Fig. 4a. The slight adsorption at low partial pressure and hysteresis loop at higher partial pressure can be observed from the shape of adsorption–desorption isotherms. Such behaviors were generally classified as type IV isotherm [30]. According to the BJH analysis, the specific surface area was 20.73 $m^2 g^{-1}$ and the pores size distribution was in the range from 2 nm to 5 nm, which was corresponding with the mesoporous microstructure.

Fig. 4b shows the magnetic hysteresis curve measured at room temperature for the CdS/MFACs (inset: the photo of magnetic separation). It can be seen that the saturation magnetization of the CdS/MFACs was 11.5 emu g^{-1}, which suggested that such composites might be easily separated from solution phase through inducing an external magnetic field.

3.5 TG curves of MFACs and CdS-MFACs

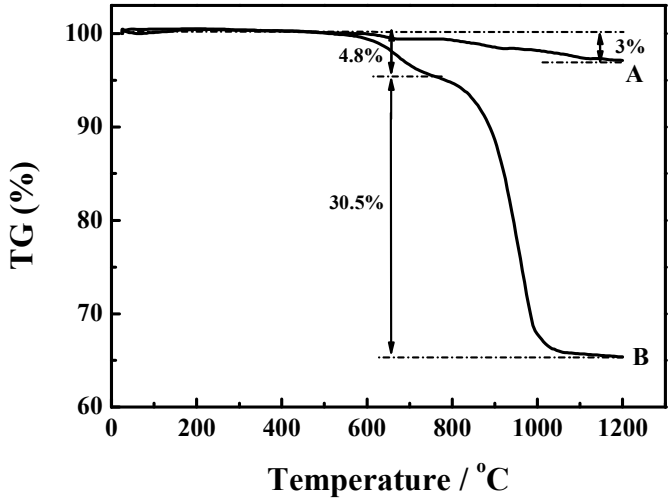

Fig. 5. TG curve of MFACs (A), TG curve of CdS-MFACs (B)

Fig. 5 shows thermogravimetric curves (TG) and of MFACS and CdS-MFACs in the temperature range from 25°C to 1200°C. Fig 5A was TG curve of MFACs, it can be seen that a little weight loss of 3%, which was perhaps caused by absorbent water, structure water and some impurity particles in MFACs, owing to MFACs are mainly composed of inorganics. For CdS-MFACs, the first stage occurred from 25°C to 735°C with weight loss of 4.8%. This may resulted from the loss of water molecules and some impurity particles in CdS-MFACs. The second stage started from 735 °C with loss of 30.5% corresponding to the decomposition of CdS nanoparticles.

3.6 Photocatalytic process

The photocatalytic activity of the CdS/MFACs was evaluated through the degradation of danofloxacin mesylate under visible light irradiation. Because of the adsorption capacity of photocatalysts had significant impacts on the degradation behavior of organic pollutants, the dynamic adsorption experiments was firstly investigated. According to the adsorption capacity of

RSC Advances Accepted Manuscript

CdS/MFACs for danofloxacin mesylate solution in dark (Fig. S3), we chosen 20 min as the dynamic adsorption time before visible light irradiation.

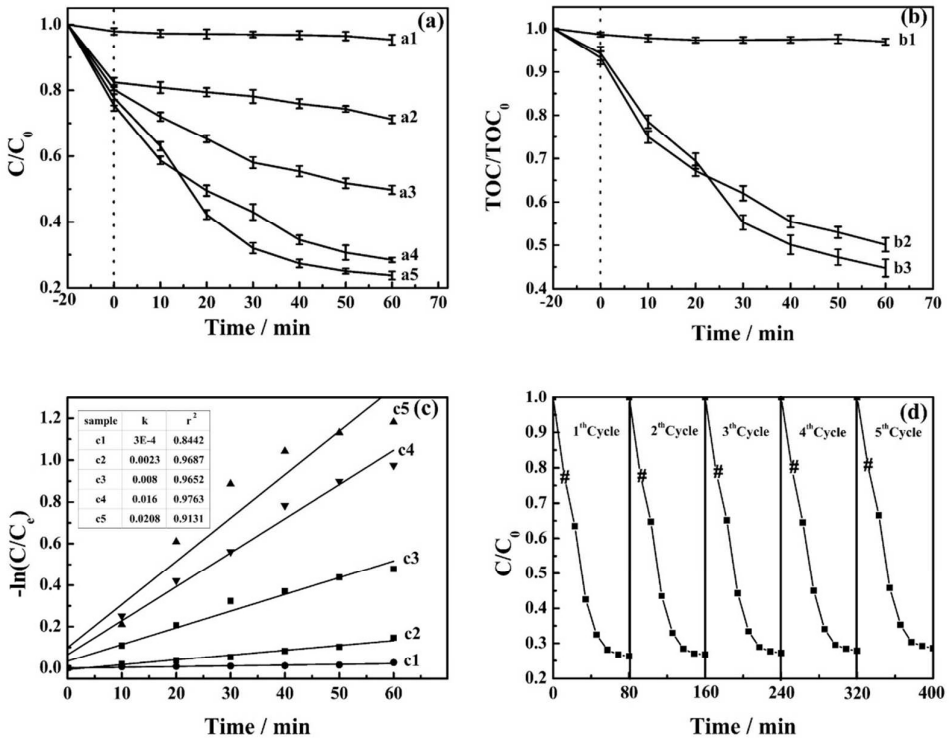

Fig. 6. Photocatalytic performances of different samples under visible light irradiation: without catalyst (a1), MFACs (a2), P25 (a3), CdS (a4), CdS/MFACs (a5) (a). TOC removal of danofloxacin mesylate: MFACs (b1), CdS (b2), CdS/MFACs (b3) (b). Kinetic plots for the photodegradation process of danofloxacin mesylate catalyzed by without catalyst (c1), MFACs (c2), P25 (c3), pure CdS (c4), CdS/MFACs (c5) (c). Repeated experiments (before (#) is stage of adsorption) (d).

Fig. 6a shows photocatalytic performances of different samples under visible light irradiation. According to the image, a blank test (danofloxacin mesylate without any catalyst) under irradiation exhibited little decrease in the concentration of danofloxacin mesylate, which meant that danofloxacin mesylate was stable under illumination. The concentration of danofloxacin mesylate in system within MFACs had some lightly changes in adsorption process, which was mainly caused by the porous structure of MFACs. Moreover, both pure CdS and CdS/MFACs showed high photocatalytic activity because of the low energy band gap of CdS. The photocatalytic degradation efficiency of CdS/MFACs reached 76.3% under the visible light irradiation within 60 min, which was higher than that of pure CdS and P25. Similar results were reported in the literature [31]. Generally, the photocatalytic reaction often occurs on the surface of the catalyst, which is directly exposed to light and the reactants [32]. Hence we conjectured that the morphology would be the main reason for the photocatalytic differences between pure CdS and CdS/MFACs and several plausible explanation for enhanced photocatalytic activity were due to: (1) when compared to pure CdS, the fly ash cenospheres makes the composites show good dispersion in danofloxacin mesylate solution, which also leads to good absorption and using of

RSC Advances Accepted Manuscript

light [33, 34]; (2) the FACs acted as a dispersing support to inhibit grain growth, which contributed to making full use of light for photocatalysis [35].

The total organic carbon (TOC) values were related to the total concentration of organic compounds in the solution, and the decrease of TOC values in irradiation time can reflect the degree of mineralization. The changes of TOC values during the degradation process of danofloxacin mesylate with CdS/MFACs were shown in Fig. 6b. The lower removal of TOC was likely attributed to the formation of simple organic compounds during the degradation of danofloxacin mesylate.

The degradation kinetics of danofloxacin mesylate were investigated by fitting the experimental data to the Langmuir–Hinshelwood model:

$$\mathrm{r} = -\frac{dC}{dt} = \frac{k_r KC}{1 + KC}$$

Because of the low concentration of reactant (the term KC→0), the Langmuir–Hinshelwood model was reduced to the pseudo first-order kinetics equation:

$$-\ln\left(\frac{C}{C_e}\right) = \mathrm{kt}$$

Where C_e represents the concentration of danofloxacin mesylate at adsorption equilibrium, C denotes the concentration at a given reaction time t, and k is the reaction rate constant determined by plotting -ln (C/C_e) vs. the reaction time t. As shown in Fig. 6c, the rate constants of different pholocatalysts were calculated to be 0.0003 min^{-1}, 0.0023 min^{-1}, 0.008 min^{-1}, 0.016 min^{-1} and 0.0208 min^{-1} for without catalyst, MFACs, P25, pure CdS and CdS/MFACs, respectively. The order of rate constants was summarized as follows: CdS/MFACs > pure CdS > P25 > MFACs > without catalyst, which were well agreement with the conclusion of the photodegradation of danofloxacin mesylate showed in the Fig. 6a. The result further illustrated the highest photocatalytic activity of CdS/MFACs.

Generally, reusability and stability were the most important factor for the practical utility of the photocatalyst. As displayed in Fig. 6d, the catalysts still remained a high photocatalytic activity without any recession during the photodegradation of danofloxacin mesylate even after 5 cycles, indicating that the CdS/MFACs was relatively stable.

4. Photocatalytic mechanism

To investigate the process of photodegradation and destruction of danofloxacin mesylate, the mass spectra of the irradiated solutions of danofloxacin mesylate at different time intervals were observed, which was shown in the supporting information (Fig. S4). When danofloxacin mesylate dissolved in water to form a solution, sulfonic acid groups were separated from the danofloxacin and danofloxacin became the main component. Consequently, a characteristic peak at 358 (the danofloxacin peak) can be seen. The probable degradation route as shown in Fig. 7. One possible scenario was that e^-_{aq} reduced at the ketone position and double bond of danofloxacin formed the alcohol product B. The process of "B to F" was because "B" lost the group of CH_3, further reaction of "B" and "F" with e^-_{aq} resulted in the formation of products of "C" and "G", which were assigned to the products of the decarboxylation. The products D and H arised from product C lost the group of $–C_3Htr_5$ and $–C_5N_2H_{11}$, respectively. Product I can be formed when product H missed –OH.

The other possibility is that danofloxacin can be generated into "E", "J" and "K" by three times successive hydroxylation. In a similar way, the product N was obtained by decarboxylation of

RSC Advances Accepted Manuscript

hydroxylation product K. The degradation processes of "K to L" and "N to O" were both of lossing the group of –F. Somewhat differently, "K to L" was a substitution process. It can form the product O if product get further oxidized. Product P was formed from "M" by missing the group of $–CH_3$. Likewise, "Q" was can be also formed from "P" by losing the groups of $–C_3H_5$ and –OH. Further the formed intermediates then were fragmented into R, S, T, U, V and other low molecular weight intermediates and finally mineralized to CO_2, H_2O and other gaseous components.

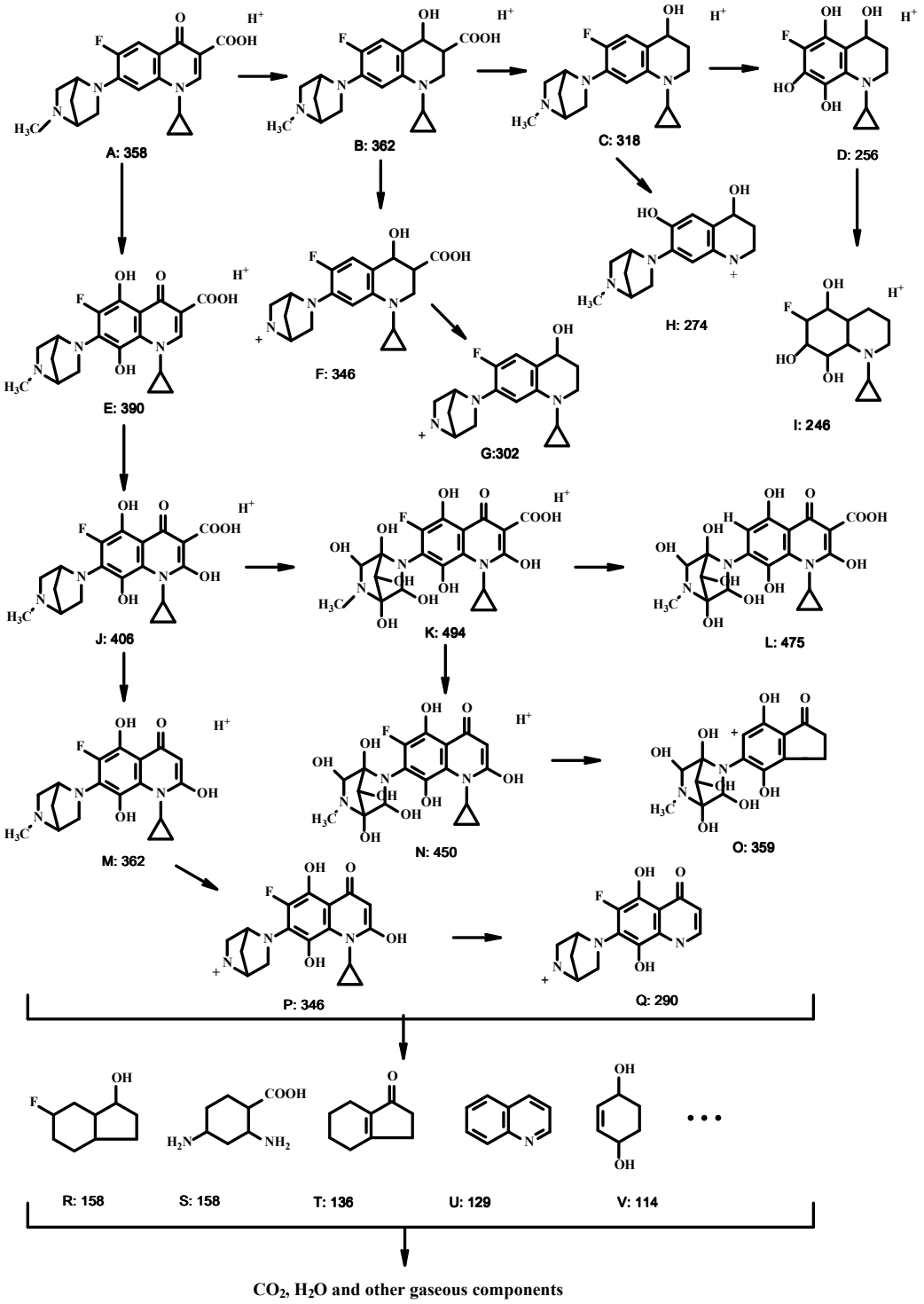

RSC Advances Accepted Manuscript

Fig. 7. The degradation course of danofloxacin mesylate.

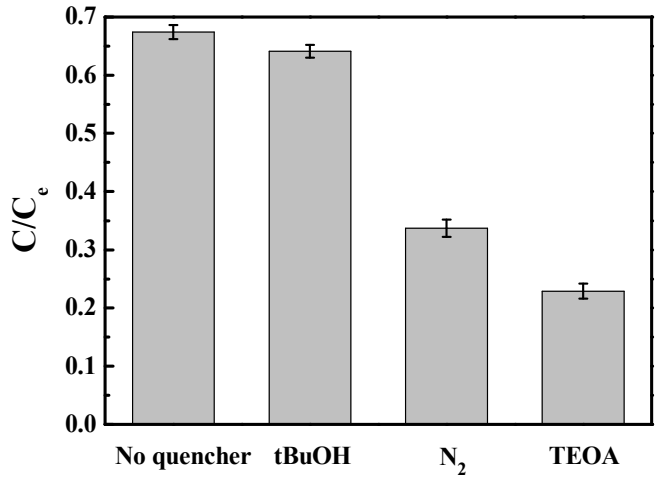

Fig. 8. Photocatalytic activities of CdS/MFACs on the degradation of danofloxacin mesylate in presence of different quenchers under visible light irradiation.

During the processes of photocatalytic degradation of danofloxacin mesylate, an array of reactive oxygen species, such as h^+, ·OH, or $\cdot O_2^-$, were supposed to be involved. In order to investigate why the CdS/MFACs was so efficient for the degradation of danofloxacin mesylate, a qualitative analysis of reactive species trapping and hydroxyl radicals were conducted. Triethanolamine (TEOA), tert-butyl alcohol (tBuOH), and N_2 acted as the quenchers for h^+, ·OH, and $\cdot O_2^-$ in the photocatalytic process, respectively. Fig.8 shows the photocatalytic activity of CdS/MFACs on the degradation of danofloxacin mesylate with different quenchers. It can be seen that the addition of tBuOH in the danofloxacin mesylate solution has little effect on the photocatalytic activity of CdS/MFACs. However, in N_2 condition, there was little oxygen in the system that limits the generation of superoxide radicals, which has a significant suppressing effect on the degradation of the danofloxacin mesylate solution. This indicates that $\cdot O_2^-$ is one of the main oxidative spcies in the degradation processes. Moreover, the photocatalytic degradation of danofloxacin mesylate is obviously inhibited after the addition TEOA, which means that h^+ was also the main active species of CdS/MFACs for the degradation of danofloxacin mesylate under visible light irradiation [36-38]. But it is not sure whether the formation of ·OH can inhibit the degradation or just have no promoting effects on the catalyst activity. Thus the followed experiment was conducted.

RSC Advances Accepted Manuscript

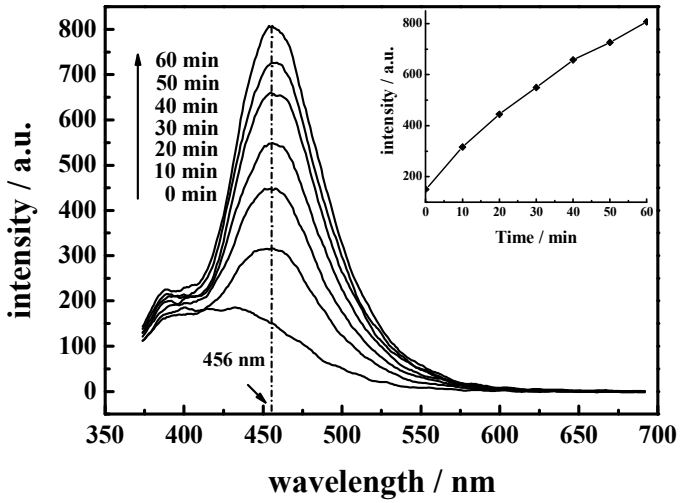

Fig. 9. Fluorescence spectral changes observed and fluorescence intensity (at 456 nm) of coumarin solution (inset) during irradiation of CdS/MFACs in 1 mM aqueous solution of coumarin (excitation at 346 nm)

As shown in Fig. 9, with the increase of irradiation time, coumarin was oxidized by the ·OH to a strong fluorescent 7-hydroxycoumarin and the fluorescence intensity continuously increased, which can be seen clearly from inset figure. This result certified that ·OH was generated by CdS/MFACs in water when it was irradiated by visible light and ·OH had no promoting effects on photocatalytic activity for the danofloxacin mesylate. Moreover, the formation of reactive radicals was further evidenced with ESR spin-trapping technique with 5,5-dimethyl-1-pyrroline-N-oxide (DMPO), which is carried out to detect the active species by visible light irradiation [39].

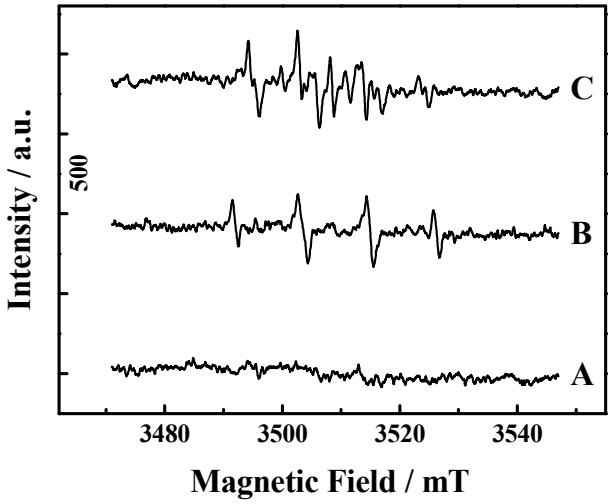

Fig. 10. DMPO spin-trapping ESR spectra of CdS/MFACs for dark (A), DMPO-•OH (B) and DMPO-$\cdot O_2^-$ under the visible light irradiation (C)

ESR spectroscopy has been frequently applied to investigate photocatalytic reactions at a molecular level. In particular, this technique has been used to follow the photoinduced generation

RSC Advances Accepted Manuscript

of charge carriers on photocatalysts and their transfer to inorganic adsorbed molecules like O_2 and H_2O. As shown in Fig. 10B, the characteristic four peaks of DMPO–·OH with intensity 1:2:2:1 are observed, which is similar to the results reported by other groups for the ·OH adduct [40], no such signals were detected in the dark. This means that irradiation is essential for generation of ·OH on the surface of the CdS/MFACs. This phenomenon further proved that ·OH existed in system. In order to detect $\cdot O_2^-$ in the system, DMSO was used to replace water. It was not only because DMSO can reduce the interference of ·OH but also the facile disproportionation of superoxide species in water precluded the slow reactions between $\cdot O_2^-$ and DMPO [41]. Fig. 10C shown the characteristic peaks, corresponding to the spin-adducts DMPO-$\cdot O_2^-$, which indicated $\cdot O_2^-$ was generated in CdS/MFACs/DMPO/DMSO system.

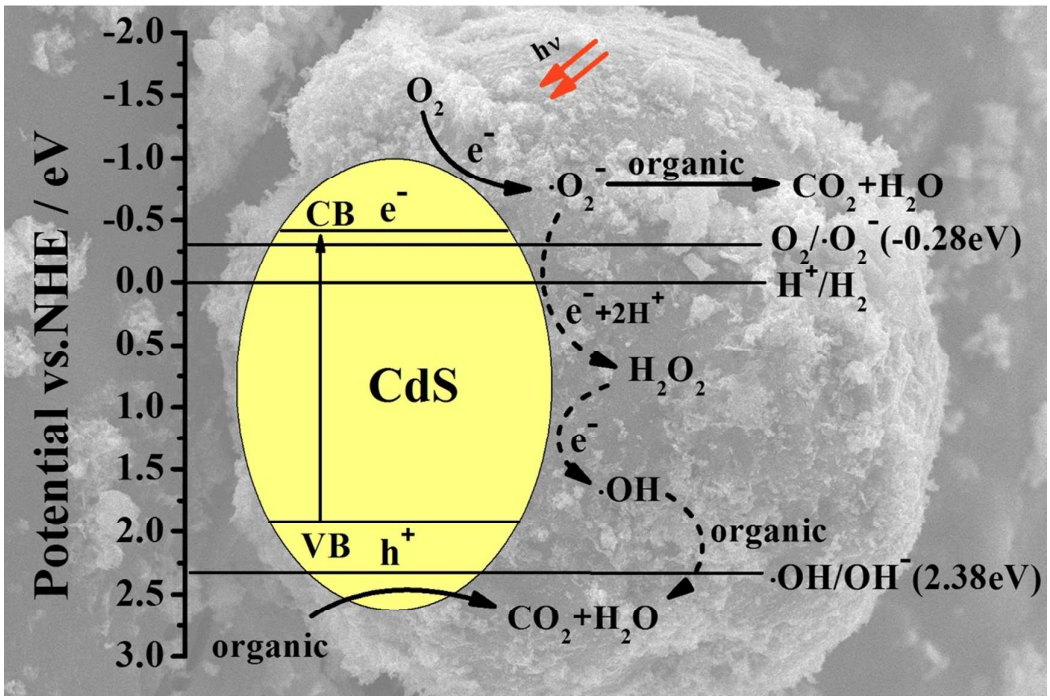

Fig. 11. Photocatalytic mechanism scheme of CdS/MFACs under visible light irradiation

Usually, ·OH and $\cdot O_2^-$ were all important redoxinitiator for photocatalytic decomposition of the organic compound [42]. Furthermore, ·OH had stronger oxidation capacity than $\cdot O_2^-$. But the main role of degradation and mineralization of danofloxacin mesylate is $\cdot O_2^-$ and h^+ rather than ·OH. In other words, the source of ·OH radicals are mainly from two ways: one was the reaction between holes and surface hydroxyl groups ($h^+ + H_2O\ (OH^-) \rightarrow \cdot OH + H^+$), and the other was the adsorbed H_2O_2 ($e^- + H_2O_2 + H^+ \rightarrow \cdot OH + H_2O$). However, in CdS/MFACs/danofloxacin mesylate system, due to the valence band edge potential of CdS (1.88 eV vs. NHE) is less positive than E°(·OH /OH^-) (2.38 eV vs.NHE), which means that the h^+ on the surface of CdS cannot oxidize OH^- to yield ·OH [43]. As depicted in Fig. 11, the conduction band of CdS (-0.52 eV) was more negative than the redox potential of $O_2/\cdot O_2^-$ (-0.28 eV), which indicated that the electrons transferred to the surface of semiconductor particles could interact with O_2 to form $\cdot O_2^-$. However, the photogenerated holes on valence band of CdS cannot result in the formation of ·OH radicals, but directly oxidize the danofloxacin mesylate. Moreover, the generation of ·OH mainly come from $\cdot O_2^-$ [44], and the possible formation process of ·OH is shown as follows:

RSC Advances Accepted Manuscript

$$\cdot O_2^- + e^- + 2H^+ \rightarrow H_2O_2$$

$$H_2O_2 + e^- \rightarrow \cdot OH + OH^-$$

Therefore, the formation quantity of ·OH was restricted by the concentration of $\cdot O_2^-$ in the system. A series of reduction-oxidation reactions would happen when part of $\cdot O_2^-$ combinated with danofloxacin mesylate, so that only small amount of ·OH formed from $\cdot O_2^-$, which corresponding with the result of the degradation experiments adding free radicals scavenger. To sum up, the photodegradation of danofloxacin mesylate over CdS/MFACs photocatalyst can be mainly affected by $\cdot O_2^-$ and the photogenerated holes on the valance bands of CdS.

5. Conclusions

The CdS/MFACs photocatalyst was successfully prepared by chemical bath deposition method. The ultraviolet visible absorption spectrum, photocatalytic activity and recycle of the CdS/MFACs were also studied. It was found that CdS/MFACs had stronger absorption, higher photocatalytic activity (76.3%) and better recycle under visible light irradiation. Furthermore, the results shown that the CdS nanoparticles are well loaded on the surface of MFACs, meanwhile CdS/MFACs composites can be quickly separated by an external magnetic field after photocatalysis. The photocatalytic mechanism was proposed based on the energy band position. By using coumarin, the changes of ·OH in CdS/MFACs photocatalysis during the reaction solution were also researched. Moreover, the free radicals can be further determined by technology of ESR and the photodegradation and mineralization of danofloxacin mesylate were mainly associated with $\cdot O_2^-$ and the photogenerated holes.

Acknowledgements

We gratefully acknowledge the natural science foundation of china (No. 21306068), the natural science foundation of jiangsu province (No. BK20130487), the financial support of china postdoctoral science foundation (No. 2012M521015) and the innovation programs foundation of jiangsu province (Nos. CXZZ13_0693 and CXZZ13_0665).

Reference

1. E. S. Elmolla and M. Chaudhuri, *Journal of hazardous materials*, 2010, **173**, 445-449.
2. L. Ji, W. Chen, S. Zheng, Z. Xu and D. Zhu, *Langmuir : the ACS journal of surfaces and colloids*, 2009, **25**, 11608-11613.
3. A. Ghauch, H. Baydoun and P. Dermesropian, *Chemical Engineering Journal*, 2011, **172**, 18-27.
4. L. Sun, C. Wang, M. Ji and X. Kong, *Chemical Engineering Journal*, 2013, **215**, 50-56.
5. Y. Yan, Y. Wu, Y. Yan, W. Guan and W. Shi, *The Journal of Physical Chemistry C*, 2013, **117**, 20017-20028.
6. C. Gadipelly, A. Pérez-González, G. D. Yadav, I. Ortiz, R. Ibáñez, V. K. Rathod and K. V. Marathe, *Industrial & Engineering Chemistry Research*, 2014, **53**, 11571-11592.
7. L. A. Silva, S. Y. Ryu, J. Choi, W. Choi and M. R. Hoffmann, *The Journal of Physical Chemistry C*, 2008, **112**, 12069-12073.
8. G. Shen and C.-J. Lee, *Crystal growth & design*, 2005, **5**, 1085-1089.
9. Q. Xiang, B. Cheng and J. Yu, *Applied Catalysis B: Environmental*, 2013, **138**, 299-303.

RSC Advances Accepted Manuscript

10. Q. Li, B. Guo, J. Yu, J. Ran, B. Zhang, H. Yan and J. R. Gong, *Journal of the American Chemical Society*, 2011, **133**, 10878-10884.
11. Q. Hao, J. Xu, X. Zhuang, Q. Zhang, Q. Wan, H. Pan, X. Zhu and A. Pan, *Materials Letters*, 2013, **100**, 141-144.
12. T. Lv, L. Pan, X. Liu and Z. Sun, *Electrochimica Acta*, 2012, **83**, 216-220.
13. C. Sriwong, S. Wongnawa and O. Patarapaiboolchai, *Chemical Engineering Journal*, 2012, **191**, 210-217.
14. B. Wang, Q. Li, W. Wang, Y. Li and J. Zhai, *Applied Surface Science*, 2011, **257**, 3473-3479.
15. H. Y. Li, S. L. Bai, Y. J. Guan and Z. B. Wang, *Advanced Materials Research*, 2012, **396**, 768-771.
16. C. Peng, X. Cheng, S. Chen, X. Li, T. Li, D. Zhang, Z. Huang and A. Zhang, *Photochemistry and photobiology*, 2012, **88**, 1433-1441.
17. B. Pan, Y. Xie, S. Zhang, L. Lv and W. Zhang, *ACS applied materials & interfaces*, 2012, **4**, 3938-3943.
18. W. Xing, L. Ni, P. Huo, Z. Lu, X. Liu, Y. Luo and Y. Yan, *Applied Surface Science*, 2012, **259**, 698-704.
19. A. Arizmendi-Morquecho, A. Chávez-Valdez and J. Alvarez-Quintana, *Applied Thermal Engineering*, 2012, **48**, 117-121.
20. Y.-t. Yu, *Powder technology*, 2004, **146**, 154-159.
21. P. Huo, Y. Yan, S. Li, H. Li and W. Huang, *Desalination*, 2010, **256**, 196-200.
22. Z. Lu, W. Zhou, P. Huo, Y. Luo, M. He, J. Pan, C. Li and Y. Yan, *Chemical Engineering Journal*, 2013, **225**, 34-42.
23. P. Gao, J. Liu, D. D. Sun and W. Ng, *Journal of hazardous materials*, 2013, **250-251**, 412-420.
24. Z. Liu, B. Wu, Y. Zhu, F. Wang and L. Wang, *Journal of colloid and interface science*, 2013, **392**, 337-342.
25. Y. Guo, X. Shi, J. Zhang, Q. Fang, L. Yang, F. Dong and K. Wang, *Materials Letters*, 2012, **86**, 146-149.
26. Z. Wang, W. Ma, C. Chen, H. Ji and J. Zhao, *Chemical Engineering Journal*, 2011, **170**, 353-362.
27. P. Huo, Z. Lu, X. Liu, X. Liu, X. Gao, J. Pan, D. Wu, J. Ying, H. Li and Y. Yan, *Chemical Engineering Journal*, 2012, **198**, 73-80.
28. S. Rengaraj, S. Venkataraj, S. H. Jee, Y. Kim, C.-w. Tai, E. Repo, A. Koistinen, A. Ferancova and M. Sillanpää, *Langmuir : the ACS journal of surfaces and colloids*, 2010, **27**, 352-358.
29. Y. Wang, H. Gao, J. Sun, J. Li, Y. Su, Y. Ji and C. Gong, *Desalination*, 2011, **270**, 258-263.
30. Z. Liu, H. Bai and D. Sun, *Applied Catalysis B: Environmental*, 2011, **104**, 234-238.
31. G. Lin, J. Zheng and R. Xu, *The Journal of Physical Chemistry C*, 2008, **112**, 7363-7370.
32. J. Wang, B. Li, J. Chen, N. Li, J. Zheng, J. Zhao and Z. Zhu, *Journal of Alloys and Compounds*, 2012, **535**, 15-20.

RSC Advances Accepted Manuscript

33. J. Lv, T. Sheng, L. Su, G. Xu, D. Wang, Z. Zheng and Y. Wu, *Applied Surface Science*, 2013, **284**, 229-234.
34. J. Zhang, H. Cui, B. Wang, C. Li, J. Zhai and Q. Li, *Applied Surface Science*, 2014, **300**, 51-57.
35. P. Sharma, V. Durga Kumari and M. Subrahmanyam, *Chemosphere*, 2008, **72**, 644-651.
36. Z. Chen, W. Wang, Z. Zhang and X. Fang, *The Journal of Physical Chemistry C*, 2013, **117**, 19346-19352.
37. T. Xu, L. Zhang, H. Cheng and Y. Zhu, *Applied Catalysis B: Environmental*, 2011, **101**, 382-387.
38. L. Ye, J. Liu, Z. Jiang, T. Peng and L. Zan, *Applied Catalysis B: Environmental*, 2013, **142-143**, 1-7.
39. C. Chen, P. Lei, H. Ji, W. Ma, J. Zhao, H. Hidaka and N. Serpone, *Environmental science & technology*, 2004, **38**, 329-337.
40. N. Zhang, S. Liu, X. Fu and Y.-J. Xu, *The Journal of Physical Chemistry C*, 2011, **115**, 9136-9145.
41. D. T. Sawyer and J. S. Valentine, *Accounts of Chemical Research*, 1981, **14**, 393-400.
42. O. Carp, *Progress in Solid State Chemistry*, 2004, **32**, 33-177.
43. H. Cheng, B. Huang, Y. Dai, X. Qin and X. Zhang, *Langmuir : the ACS journal of surfaces and colloids*, 2010, **26**, 6618-6624.
44. M. R. Hoffmann, S. T. Martin, W. Choi and D. W. Bahnemann, *Chemical reviews*, 1995, **95**, 69-96.

RSC Advances Accepted Manuscript

A table of contents entry

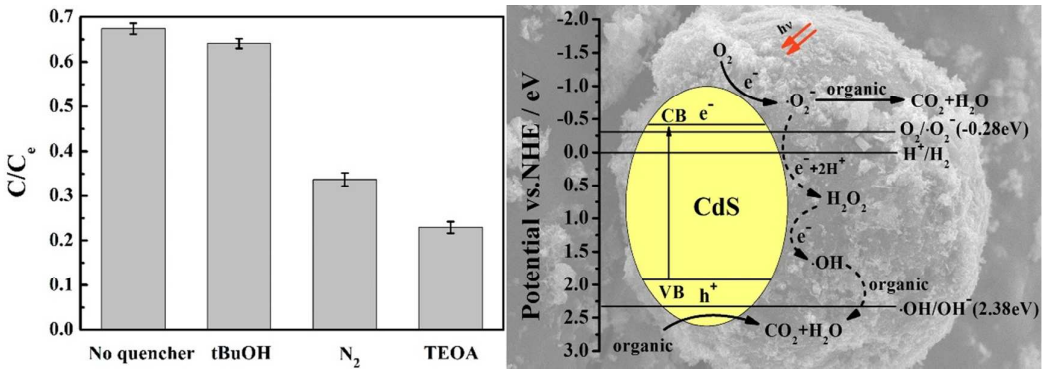

Photocatalysts easily recycled with magnetic fly ash cenospheres as the carrier, the effects of free radicals are discussed in detail.

RSC Advances Accepted Manuscript